

# co-BPM: a Bayesian Model for Estimating Divergence and Distance of Distributions

Kun Yang<sup>1</sup>, Hao Su<sup>2</sup>, and Wing Hung Wong<sup>3</sup>

<sup>1</sup>Institute of Computational and Mathematical Engineering, Stanford  
University

<sup>2</sup>Department of Computer Science, Stanford University

<sup>3</sup>Department of Statistics, Stanford University

<sup>3</sup>Department of Health Research and Policy, Stanford University

## Abstract

A Bayesian model is proposed to characterize the discrepancy of two samples, e.g., to estimate the divergence or distance of their underlying distributions. The core idea of this framework is to learn a partition of the sample space that best captures the landscapes of their distributions. In order to avoid the pitfalls of plug-in methods that estimate each sample density independently with respect to the Lebesgue measure, we make direct inference on the two distributions simultaneously from a joint prior, i.e., the coupled binary partition prior. Our prior leverages on the class of piecewise constant functions built upon binary partitions of the domain. Our model ushers a unified

way to estimate various types of discrepancies between samples and enjoys convincing accuracy. We demonstrate its effectiveness through simulations and comparisons.

**Key Words:** coupled binary partition, divergence, MCMC, variance reduction

## 1 Introduction

How to understand the discrepancy between two samples is of fundamental importance in various disciplines such as statistics, information theory and machine learning. In statistics, hypothesis testing procedures such as Kolmogorov-Smirnov test and Cramer-von Mises test are based on some discrepancy measurement of the empirical distributions, and a common goal in Bayesian experimental design [2] is to maximize the expected Kullback-Leibler (KL) divergence between the prior and the posterior. In information theory, divergence plays an important role since other information theoretic quantities such as mutual information and Shannon Entropy are derived from it. In machine learning, probability distance measures such as Total Variation, Hellinger Distance and KL divergence are often applied as a loss function in evaluation and optimization of the density estimation algorithms. Moreover, distribution discrepancies can also be applied to image registration and multimedia classification problems as a similarity measure [4].

Estimating discrepancies of two probability distributions, especially KL divergence, based on a set of samples from each distribution has a long history and rich literature. For ease of elaboration, we formulate the problem in mathematical terms: given the sample space  $\Omega$ , two sets of i.i.d samples  $\mathcal{X} = \{x_i\}_{i=1}^{n_1}$  and  $\mathcal{Y} = \{y_i\}_{i=1}^{n_2}$  are generated from probability measures  $P_1$  and  $P_2$  with densities  $p_1(x)$  and  $p_2(y)$  respectively. Various measures of discrepancy of  $p_1$  and  $p_2$  are often one of the following three forms:

1.  $D_\phi(p_1, p_2) = \int p_1(x) \phi\left(\frac{p_2(x)}{p_1(x)}\right) dx$ , where  $\phi$  is a convex function.  $D_\phi$  is the class of Ali-Silvey distances [1], also known as  $f$ -divergences. As a special case, KL divergence corresponds to  $\phi(x) = -\log(x)$ .
2.  $D_\alpha(p_1, p_2) = \frac{1}{\alpha-1} \log \int \frac{p_1(x)^\alpha}{p_2(x)^{\alpha-1}} dx$ , where  $\alpha$  is a positive constant.  $D_\alpha$  is the Rényi divergence [11] of order  $\alpha$  or  $\alpha$ -divergence. The degenerated case, i.e.,  $\alpha = 1$ , is the KL divergence.
3.  $D_q(p_1, p_2) = \left(\frac{1}{2} \int |p_1(x)^{\frac{1}{q}} - p_2(x)^{\frac{1}{q}}|^q dx\right)^{\frac{1}{q}}$ , where  $q = 1$  is the total variation distance and  $q = 2$  is the Hellinger distance.

When necessary, we use  $D$  to represent  $D_\phi$ ,  $D_\alpha$  and  $D_q$  to simplify notations.

We are interested in estimating  $D$  from sample sets  $\mathcal{X}$  and  $\mathcal{Y}$ , without any prior knowledge of  $p_1$  and  $p_2$ . A conceptually simple approach is to proceed in two-steps: estimate the densities  $\hat{p}_1$  and  $\hat{p}_2$  according to the  $\mathcal{X}$  and  $\mathcal{Y}$  independently then calculate  $D(\hat{p}_1, \hat{p}_2)$ . However, this method is unattractive for the following reasons: i) multivariate density estimation itself is a challenging problem and often more difficult than comparing distributions, so poorly estimated densities can cause subsequent discrepancy estimation to suffer from high variance and bias; ii) if the first stage is carried out independently, there is no easy way to compute their discrepancy  $D(\hat{p}_1, \hat{p}_2)$  analytically; some numeric or approximation routines have to be employed, which in turn introduce more error terms. Hence, throughout this paper, we focus on the class of single-shot methods, i.e., comparing samples directly and simultaneously.

In this paper, we introduce a single-shot Bayesian model, which we name as **coupled Binary Partition Model** (co-BPM). Our model design is inspired by two key ideas. First, we use an adaptive partitioning scheme, which has been demonstrated to be more scalable

(see Table 1) than traditional domain splitting methods such as histogram [15] or regular paving [12]. Second, instead of partitioning based upon  $\mathcal{Y}$  alone as in [15], we force the domain  $\Omega$  to be *coupled* so that it is partitioned with respect to  $\mathcal{X}$  and  $\mathcal{Y}$  simultaneously. Therefore, our model is capable of capturing the landscape of both  $\mathcal{X}$  and  $\mathcal{Y}$ , thus is more effective in estimating their discrepancies. As a second consequence, this coupled scheme also provides a unified framework to estimate three families of discrepancies.

We highlight our contributions as follows:

1. To our knowledge, co-BPM is the first *single-shot domain-partition* based Bayesian model for discrepancy estimation, that is scalable in both dimension and sample size.
2. The specifically tailored MCMC sampling algorithm exploits the sequential buildup of binary partition for rapid mixing.
3. The method is tested in *higher dimensional* settings that are rare in previous work. Experiments show that we achieve fast convergence and high accuracy.
4. We propose two *variance reduction* approaches that are effective for discrepancies involving divisions (e.g., in  $\alpha$ -divergence).

We validate our model by intensive simulations: 1) two sanity tests are used to demonstrate that our model is sensitive to the differences among samples; 2) a 4-dim example is used to demonstrate the effectiveness of variance reduction; 3) higher dimensional examples in 5-dim and 10-dim are carried out and are compared to standard Kernel Density Estimator.

## 2 Related Work

We review several methods in the context of information theory and machine learning. Interested readers may refer to [13, 16, 6, 10, 8] for other recent developments. In [15], Wang et al. proposes a domain-splitting method that constructs an adaptive partition of the sample space with respect to  $\mathcal{Y}$ , then Radon-Nikodym derivative  $p_1(x)/p_2(x)$  can be estimated with empirical probability mass (with the correction term on the boundary) in each sub-region. In 1-dimension, strong consistency is established and several algorithmic refinements are suggested. In high dimensions, a partitioning scheme is also mentioned based on the heuristics in 1-dimensional case, however, there are not enough numeric simulations to justify the heuristics. In [9], Nguyen et al. derives a variational characterization of the  $f$ -divergence in terms of a Bayes decision problem, which is exploited to develop an  $M$ -estimator. The theoretical results of consistency and convergence rates are provided. It is also shown that the estimation procedure can be casted into a finite-dimensional convex program and solved efficiently when the function class is defined by reproducing kernel Hilbert spaces. In [14], least-squares density-difference (LSDD) estimator is developed in the framework of kernel regularized least-squares estimation. The finite sample error bound shows that LSDD achieves the optimal convergence rate. They also demonstrate several pattern recognition applications.

Despite of the success of these methods, they are insufficient in many scenarios. For example, since  $\mathcal{X}$  and  $\mathcal{Y}$  are random samples, one may be interested in the confidence (credible) intervals of estimated discrepancies [13], but deriving such quantities are non-trivial for these methods. Secondly, these methods and theories are all set up for a specific type of discrepancy and are usually not directly applicable to others. Moreover, to the best of our knowledge, there is little work on tackling discrepancy estimation under the

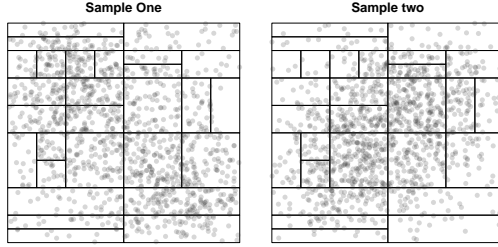


Figure 1: An illustration of **joint binary partition** of two samples through the coupled binary partition model.

Bayesian perspective. In contrast, co-BPM provides natural solutions to the above issues and demonstrates its superiority in terms of scalability.

### 3 Notation and Preliminaries

Throughout the paper, we assume  $\Omega = [0, 1]^d$  and consider the domain-splitting approach to estimate the discrepancies through coordinate-wise binary partition (Figure 1). A binary partition has hierarchical structure that is constructed sequentially: starting with  $\mathcal{B}_1 = \{r_{1,1} = \Omega\}$  at level 1, action  $a_1$  is taken to split  $\Omega$  into  $\mathcal{B}_2 = \{r_{1,2}, r_{1,2}\}$  along the middle of one of its coordinates; then at level 2, action  $a_2$  is taken to split one of sub-rectangles in  $\mathcal{B}_2$  into  $\mathcal{B}_3 = \{r_{1,3}, r_{2,3}, r_{3,3}\}$  evenly. The process keeps on till the specified level is reached. Given the maximum level  $l$ , the action sequence is denoted as  $A_l = (a_1, \dots, a_{l-1})$ .  $A_l$  uniquely determines a split of  $\Omega$ , which is denoted as  $\{r_{1,l}, \dots, r_{l,l}\}$ . It is necessary to point out that multiple action sequences may result in the same partition. An important property of binary partition motivates our coupling scheme in the following section.

**Property 1.** *For any pair of action sequences  $A_{l_1}$  and  $A_{l_2}$  and their partitions  $\{r_{i,l_1}\}_{i=1}^{l_1}$  and  $\{r_{i,l_2}\}_{i=1}^{l_2}$ , there exists a sequence  $A_l$  and its partition  $\{r_{i,l}\}_{i=1}^l$  such that  $r_{i,l_k}$  is the union of a subset of  $\{r_{i,l}\}_{i=1}^l$  for  $k = 1, 2$  and  $i = 1, \dots, l_k$ , namely,  $A_l$  defines a more refined partition*

than  $A_{l_1}$  or  $A_{l_2}$ .

The next theorem shows that a partition of  $\Omega$  gives a lower bound of the discrepancies.

**Theorem 1.** *Given a partition  $\{r_{1,l}, \dots, r_{l,l}\}$  of  $\Omega$  at level  $l$ , let*

$$\tilde{p}_i(x) = \sum_{k=1}^l \frac{P_i(r_{k,l})}{|r_{k,l}|} \mathbf{1}\{x \in r_{k,l}\}$$

where  $i = 1, 2$  and  $|\cdot|$  denotes the volume or size, then

$$D(p_1, p_2) \geq D(\tilde{p}_1, \tilde{p}_2) \tag{1}$$

namely, a partition gives a unified way to estimate  $D$ .

*Remark 3.1.* Another lower bound [9] of  $D_\phi$  is  $\sup_{f \in \mathcal{F}} \int [f dP_2 - \phi^*(f) dP_1]$ , where  $\mathcal{F}$  is a class of functions and  $\phi^*$  is the conjugate dual function of  $\phi$ . Theorem 1 shifts the difficulty of estimation from finding a good  $\mathcal{F}$  to a good partition.

*Remark 3.2.* By the definition of Riemann integral, it is trivial to show that  $D(p_1, p_2) = \sup D(\tilde{p}_1, \tilde{p}_2)$ , where the supremum is taken over all possible partitions on all levels.

We present the proof for  $D_\phi$  here and leave the proof for  $D_\alpha$  and  $D_q$  in the appendix.

*Proof.* For  $D_\phi$ , we decompose the integral by  $\{r_{1,l}, \dots, r_{l,l}\}$  and apply Jensen's inequality,

$$\begin{aligned} D_\phi(p_1, p_2) &= \int_{\Omega} p_1(x) \phi\left(\frac{p_2(x)}{p_1(x)}\right) dx = \sum_{i=1}^l \int_{r_{i,l}} p_1(x) \phi\left(\frac{p_2(x)}{p_1(x)}\right) dx \\ &= \sum_{i=1}^l P_1(r_{i,l}) E_{p_1(\cdot|r_{i,l})} \left[ \phi\left(\frac{p_2(x)}{p_1(x)}\right) \right] \geq \sum_{i=1}^l P_1(r_{i,l}) \phi\left( E_{p_1(\cdot|r_{i,l})} \frac{p_2(x)}{p_1(x)} \right) = \sum_{i=1}^l P_1(r_{i,l}) \phi\left( \frac{P_2(r_{i,l})}{P_1(r_{i,l})} \right) \end{aligned} \tag{2}$$

□

$\Omega_{12}$	$\Omega_{21}$	$\Omega_{22}$
$\Omega_{11}$		

	$D_{q=1}$	$D_{q=2}$	$D_{\alpha=1}$	$D_{\alpha=2}$
Hist	0.5269	0.4935	0.7964	1.0291
BP	<b>0.5431</b>	<b>0.4990</b>	<b>0.8267</b>	<b>1.0527</b>
Truth	0.5518	0.5204	0.8604	1.0769

Table 1: **A simple illustration demonstrates the importance of a good partition.** (I)  $\mathcal{B}_1 = \{\Omega_{11}, \Omega_{12}\}$  and  $\mathcal{B}_2 = \{\Omega_{21}, \Omega_{22}\}$  are two partitions of unit cube. Consider  $p_1(x) = \frac{3}{2}\mathbf{1}\{x \in \Omega_{11}\} + \frac{1}{2}\mathbf{1}\{x \in \Omega_{12}\}$  and  $p_2(x) = \frac{1}{2}\mathbf{1}\{x \in \Omega_{11}\} + \frac{3}{2}\mathbf{1}\{x \in \Omega_{12}\}$ . Under  $\mathcal{B}_1$ , the lower bounds equal  $D(p_1, p_2)$ , i.e.,  $D_\phi = \frac{3}{4}\phi(\frac{1}{3}) + \frac{1}{4}\phi(3)$ ,  $D_{q=1} = \frac{1}{2}$ ,  $D_{q=2} = \frac{\sqrt{3}}{2} - \frac{1}{2}$ ,  $D_\alpha = \frac{1}{\alpha-1} \log(\frac{3}{4} \cdot 3^{\alpha-1} + \frac{1}{4} \cdot \frac{1}{3}^{\alpha-1})$  respectively; however, under  $\mathcal{B}_2$ , the lower bounds are  $\phi(1)$ , 0, 0, 0 respectively. (II)  $p_1(x) = \beta_{3,5}(x_1)\beta_{3,5}(x_2)$  and  $p_2(x) = \mathbf{1}\{x \in [0, 1]^2\}$ . On the left is histogram by dividing each dimension into 8 equal sub-intervals; on the right is an adaptive partition with 64 sub-rectangles. As summarized in the right table, **BP** (adaptive binary partition) is closer to **Truth** (the true values) than **Hist** (histogram).

Remark 3.2 indicates the divergence can be defined over countable partitions. Since we attempt to approximate  $D(p_1, p_2)$  by  $D(\tilde{p}_1, \tilde{p}_2)$  from some finite partitioning, this inequality implies the importance of a good partition. A simple illustration is given in Table 1.

A closer look into the proof of Theorem 1 gives us more insights. Let's take the derivation for  $D_\phi$  as an example. Within each region, the gap between  $D(p_1, p_2)$  and  $D(\tilde{p}_1, \tilde{p}_2)$  comes from applying Jensen's inequality, therefore, it can be closed if  $p_1(x)/p_2(x)$  in each region is approximately constant. Similar observations can be found from other types of  $D$ , as well. Such observations indicate that partitioning the domain more finely would reduce the estimation bias. However, an overly fine partitioning will cause insufficient samples in each region and inadvertently increase the overall estimation variance. So there is a *trade-off between bias and variance*. Therefore, an appropriate partitioning respecting the tradeoff should reflect the landscape of  $\mathcal{X}$  and  $\mathcal{Y}$  simultaneously and avoid over-cutting. We will see how this intuition is implemented in our Bayesian model.



## 4 Coupled Binary Partition Model

In light of Theorem 1 and the importance of partitions, we model probability mass pairs  $(P_1(r_{i,l}), P_2(r_{i,l}))_{i=1}^l$  directly for a given partition  $\{r_{i,l}\}_{i=1}^l$ . Since the lower bounds (1) need only  $(P_1(r_{i,l}), P_2(r_{i,l}))_{i=1}^l$ , once they are fixed, we restrict the density in each sub-rectangle to be constant to reduce the complexity of density class, i.e., the density class is piecewise constant functions supported on binary partitions.

Specifically, the prior is constructed as follows: 1) given the deepest level  $L^1$ , the action sequence of level  $l \leq L$  has a prior density proportional to  $\exp(-\sigma l)$  with some positive  $\sigma$  and that all sequences at the same level are distributed uniformly; 2) given an action sequence  $A_l = (a_1, \dots, a_{l-1})$  and the fact that  $\sum_{i=1}^l P_k(r_{i,l}) = 1$  for  $k = 1, 2$ , the probability masses  $(P_1(r_{i,l}))_{i=1}^l, (P_2(r_{i,l}))_{i=1}^l$ , denoted as  $\mathbf{m}_{1,l}, \mathbf{m}_{2,l}$  or  $(m_{1i,l})_{i=1}^l, (m_{2i,l})_{i=1}^l$  have a Dirichlet prior  $\text{Dir}(\delta, \dots, \delta)$  respectively with some positive  $\delta$  and the priors are independent between samples  $\mathcal{X}$  and  $\mathcal{Y}$ . Thus,

$$p(l, A_l, (\mathbf{m}_{1,l}, \mathbf{m}_{2,l})) \propto \exp(-\sigma l) \prod_{i=1}^l m_{1i,l}^{\delta-1} \prod_{i=1}^l m_{2i,l}^{\delta-1}$$

The densities are uniform conditioned on each sub-rectangle, i.e.,

$$\hat{p}_1(x) = \sum_{i=1}^l \frac{m_{1i,l}}{|r_{i,l}|} \mathbf{1}\{x \in r_{i,l}\}, \hat{p}_2(y) = \sum_{i=1}^l \frac{m_{2i,l}}{|r_{i,l}|} \mathbf{1}\{y \in r_{i,l}\}$$

As discussed in Section 1, a naive two step algorithm proceeds as follows: estimating two piecewise constant densities  $\hat{p}_1$  and  $\hat{p}_2$  supported on (different) binary partitions independently based on  $\mathcal{X}$  and  $\mathcal{Y}$ ; then computing  $D(\hat{p}_1, \hat{p}_2)$ , which requires to consider all the

---

<sup>1</sup> $L$  has negligible impact on the model (just pick a very large  $L$ ). The reason we set the deepest level is to make sure that it is a *proper prior* since there are finite number of partitions for a given level.

intersections of sub-rectangles between two partitions. The drawbacks of this type of approach are already discussed. However, according to Property 1, any two piecewise constant densities supported on different binary partitions can be rewritten such that they are defined on the same binary partition, thus we *couple*  $\hat{p}_1, \hat{p}_2$  by forcing the same  $A_l$  in the prior such that Theorem 1 is applicable. The difference of  $\hat{p}_1, \hat{p}_2$  is captured by  $\mathbf{m}_{1,l}, \mathbf{m}_{2,l}$ .

The likelihood of  $\mathcal{X}$  and  $\mathcal{Y}$  is

$$p(\mathcal{X}, \mathcal{Y} | (l, A_l, (\mathbf{m}_{1,l}, \mathbf{m}_{2,l}))) = \prod_{i=1}^l \left( \frac{m_{1i,l}}{|r_{i,l}|} \right)^{n_{1i,l}} \prod_{i=1}^l \left( \frac{m_{2i,l}}{|r_{i,l}|} \right)^{n_{2i,l}}$$

where  $(n_{ki,l})_{i=1}^l, k = 1, 2$  denotes the number of points in each region for samples  $\mathcal{X}, \mathcal{Y}$ . Under our assumption, the prior of  $(\mathbf{m}_{1,l}, \mathbf{m}_{2,l})$  is distributed with joint Dirichlet distribution  $\text{Dir}(\delta, \dots, \delta) \times \text{Dir}(\delta, \dots, \delta)$ . By denoting  $\Theta = (l, A_l, (\mathbf{m}_{1,l}, \mathbf{m}_{2,l}))$ , the posterior is

$$\begin{aligned} p(\Theta = (l, A_l, (\mathbf{m}_{1,l}, \mathbf{m}_{2,l})) | \mathcal{X}, \mathcal{Y}) &\propto p(\Theta) p(\mathcal{X}, \mathcal{Y} | \Theta) \\ &\propto \exp(-\sigma l) \prod_{i=1}^l \left( \frac{1}{|r_{i,l}|} \right)^{n_{1i,l} + n_{2i,l}} \prod_{i=1}^l (m_{1i,l})^{\delta + n_{1i,l} - 1} \prod_{i=1}^l (m_{2i,l})^{\delta + n_{2i,l} - 1} := \psi(\Theta | \mathcal{X}, \mathcal{Y}) \end{aligned} \quad (3)$$

Through sampling from the posterior, the discrepancies are estimated by  $D(\hat{p}_1, \hat{p}_2)$ .

## 4.1 Sampling

According to the decomposition in (3), the probability masses and the decision sequence are sampled hierarchically. The first step is to generate the level  $l$  and actions  $A_l$ . By marginalizing  $\mathbf{m}_{1,l}$  and  $\mathbf{m}_{2,l}$  in (3),  $(A_l, l)$  is distributed as

$$p(A_l, l | \mathcal{X}, \mathcal{Y}) \propto \exp(-\sigma l) \beta((\delta + n_{1i,l})_{i=1}^l) \beta((\delta + n_{2i,l})_{i=1}^l) \prod_{i=1}^l \left( \frac{1}{|r_{i,l}|} \right)^{n_{1i,l} + n_{2i,l}} \quad (4)$$

where  $\beta(\cdot)$  is the multinomial Beta function. Furthermore, conditioned on  $l$ ,  $A_l$  is distributed as

$$p(A_l|l, \mathcal{X}, \mathcal{Y}) \propto \beta((\delta + n_{1i,l})_{i=1}^l) \beta((\delta + n_{2i,l})_{i=1}^l) \prod_{i=1}^l \left( \frac{1}{|r_{i,l}|} \right)^{n_{1i,l} + n_{2i,l}} \quad (5)$$

once  $A_l$  is generated,  $\mathbf{m}_{1,l}$  and  $\mathbf{m}_{2,l}$  are sampled through  $\text{Dir}((\delta + n_{1i,l})_{i=1}^l)$  and  $\text{Dir}((\delta + n_{2i,l})_{i=1}^l)$  respectively.

It is impossible to obtain the analytical distribution of  $(A_l, l)$ , Markov Chain Monte Carlo is employed to sample the posterior (3). However, given the vast parameter space and the countless local modes, the naive Metropolis-Hastings [3] suffers from a waiting time dilemma [7]. In order to sample effectively, a proposal function should be chosen with the two properties: 1) it reflects the structure of binary partition and the proposed partition is generated with respect to  $\mathcal{X}$  and  $\mathcal{Y}$  for rapid mixing; 2) the corresponding acceptance ratio depends on a smaller set of parameters; in other words, the transition probability is controlled by a subset of  $\Theta$ , such that the size (dimensionality) of searching space is reduced. Define

$$g(\Theta' = (l', A_{l'}, (\mathbf{m}_{1,l'}, \mathbf{m}_{2,l'})) | \Theta = (l, A_l, (\mathbf{m}_{1,l}, \mathbf{m}_{2,l}))) = p(A_{l'}, l' | A_l, l) p((\mathbf{m}_{1,l'}, \mathbf{m}_{2,l'}) | A_{l'}, l)$$

where  $p(A_{l'}, l' | A_l, l) = p(l' | l) p(A_{l'} | A_l)$  defines the jump probability and  $l'$  is constraint to be  $l - 1$  and  $l + 1$ . In order to exploit the sequential structure of binary partition such that each  $a_l$  is drawn with the guidance of  $A_l$ ,  $p(A_{l+1} | A_l) = p(a_l | A_l)$  is defined as

$$\begin{aligned} p(a_l | A_l) &= \frac{p(A_{l+1} | l + 1, \mathcal{X}, \mathcal{Y})}{p(A_l | l, \mathcal{X}, \mathcal{Y})} \\ &\propto \frac{\beta((\delta + n_{1i,l+1})_{i=1}^{l+1}) \beta((\delta + n_{2i,l+1})_{i=1}^{l+1})}{\beta((\delta + n_{1i,l})_{i=1}^l) \beta((\delta + n_{2i,l})_{i=1}^l)} \frac{\prod_{i=1}^l |r_{i,l}|^{n_{1i,l} + n_{2i,l}}}{\prod_{i=1}^{l+1} |r_{i,l+1}|^{n_{1i,l+1} + n_{2i,l+1}}} \end{aligned} \quad (6)$$

and  $p(A_{l-1}|A_l) = p(l-1|l)$ ;  $p((\mathbf{m}_{1,l'}, \mathbf{m}_{2,l'})|A_{l'}, l')$  is the joint Dirichlet distribution  $\text{Dir}((\delta + n_{1i,l'})_{i=1}^{l'}) \times \text{Dir}((\delta + n_{2i,l'})_{i=1}^{l'})$ . Thus, the acceptance ratio is

$$Q(\Theta \rightarrow \Theta') = \min\left\{1, \frac{\psi(\Theta')g(\Theta|\Theta')}{\psi(\Theta)g(\Theta'|\Theta)}\right\} = \min\left\{1, \frac{\exp(\sigma l) \prod_{i=1}^l |r_{i,l}|^{n_{1i,l}+n_{2i,l}} p(A_l, l|A_{l'}, l') \beta((\delta + n_{1i,l'})_{i=1}^{l'}) \beta((\delta + n_{2i,l'})_{i=1}^{l'})}{\exp(\sigma l') \prod_{i=1}^{l'} |r_{i,l'}|^{n_{1i,l'}+n_{2i,l'}} p(A_{l'}, l'|A_l, l) \beta((\delta + n_{1i,l})_{i=1}^l) \beta((\delta + n_{2i,l})_{i=1}^l)}\right\} \quad (7)$$

where  $\mathcal{X}, \mathcal{Y}$  are omitted to simplify notations. According to (7),  $\mathbf{m}_{1,l}, \mathbf{m}_{1,l'}$  and  $\mathbf{m}_{2,l}, \mathbf{m}_{2,l'}$  are canceled,  $Q(\Theta \rightarrow \Theta')$  depends on  $(A_l, l)$  and  $(A_{l'}, l')$  solely and avoids to searching the vast space of probability masses. Moreover, if  $p(l'|l)$  is chosen to be symmetric,  $Q(\Theta \rightarrow \Theta')$  can be further simplified.

In higher dimensions, sampling according to  $p(A_{l'}|A_l)$  requires to count the number of points of  $\mathcal{X}, \mathcal{Y}$  in each sub-rectangle of  $A_{l'}$ , which is expensive (with complexity  $O((n_1 + n_2)d)$ ). If we are willing to run longer chains with cheaper cost per iteration, another heuristic choice for transition  $p(A_{l'}, l'|A_l, l)$  is to increase or shrink  $A_l$  by one uniformly:  $p(A_{l+1}, l+1|A_l, l) = p(l+1|l)/(2l \cdot d)$  and  $p(A_{l-1}, l-1|A_l, l) = p(l-1|l)$  for  $1 < l < L$ ;  $p(A_2, 2|A_1, 1) = 1/d$  and  $p(A_{L-1}, L-1|A_L, L) = 1$  on the boundary.

## 5 Numeric Simulations

**Sanity Tests.** We use two ‘‘sanity tests’’ to demonstrate that our model is sensitive to differences among samples. The first group  $p_{11}$  and  $p_{12}$  are chosen because the mixture of  $p_{11}$  and  $p_{12}$  is uniformly distributed, i.e.,  $\frac{1}{2}(p_{11} + p_{12}) = \mathbf{1}\{x \in [0, 1]^2\}$ ; we generate 1,000 points each, thus the combined sample is equivalent to 2,000 points from uniform distribution; as shown in the first row of Figure 2, their difference is revealed by the partition well. The

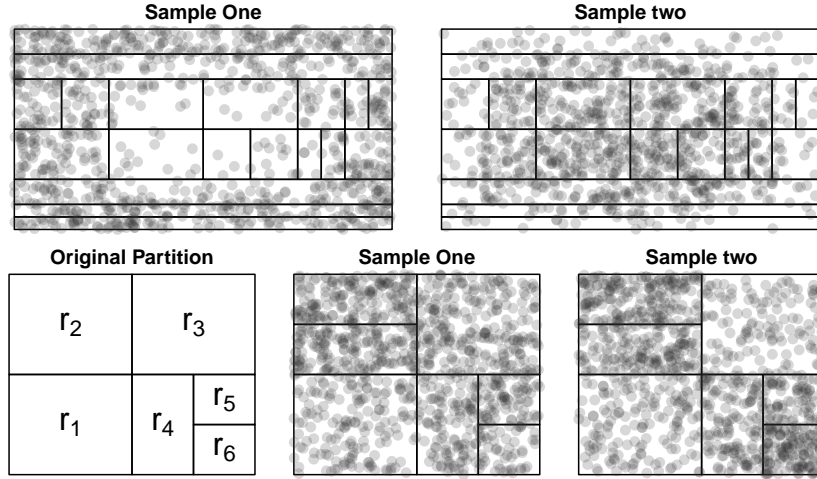


Figure 2: **Sanity Tests.** First row: 1,000 samples drawn from  $p_{11}$  and  $p_{21}$  and the learned partition; second row: 1,000 samples drawn from  $p_{21}$  and  $p_{22}$  and the learned partition.

second group  $p_{21}$  and  $p_{22}$  are chosen such that they are both supported on the binary partition and  $p_{22}$  is defined on a finer partition than  $p_{21}$ ; a good model should be able to produce the underlying partition, i.e., find a density that is finer than both densities; the second row of Figure 2 shows this result.

$$p_{11}(x) = \frac{9}{5}\mathbf{1}\{x \in [0, 1]^2\} - \frac{4}{5}\beta_{2,2}(x_1)\beta_{2,2}(x_2), p_{12}(x) = \frac{1}{5}\mathbf{1}\{x \in [0, 1]^2\} + \frac{4}{5}\beta_{2,2}(x_1)\beta_{2,2}(x_2)$$

$$p_{21}(x) = \frac{2}{3}\mathbf{1}\{x \in r_1\} + \frac{4}{3}\mathbf{1}\{x \in r_2\} + \mathbf{1}\{x \in r_3 \cup r_4 \cup r_5 \cup r_6\}$$

$$p_{22}(x) = \frac{2}{3}\mathbf{1}\{x \in r_1\} + \frac{4}{3}\mathbf{1}\{x \in r_2\} + \frac{1}{2}\mathbf{1}\{x \in r_3\} + \mathbf{1}\{x \in r_4\} + \frac{4}{3}\mathbf{1}\{x \in r_5\} + \frac{8}{3}\mathbf{1}\{x \in r_6\}$$

**Simple Examples.** We demonstrate our methods by 3 simulations with dimension  $d = 1, 2, 3$  and size  $n_1 = n_2 = 50, 250, 1250$ . The parameters for co-BPM are,  $L = 50000$ ,  $\delta = 1/2$  (which is the Jeffrey's non-informative prior),  $\sigma = d + 1$ ,  $p(l + 1|l) = p(l - 1|l) = 1/2$  for  $1 < l < L$  and  $p(L - 1|L) = 1$ ,  $p(2|1) = 1$  on the boundary. The number of replicas for the

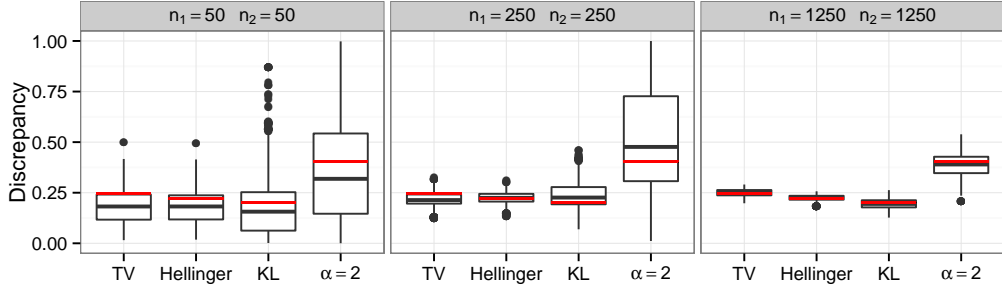


Figure 3: **1-dimensional simulation.** We draw 8,000 samples and generate box-plot after discarding the first 5,000 burn-in samples. Theoretical discrepancies (red lines): 0.2461, 0.2207, 0.2000, 0.4056.

box-plot is 3,000 and the burn-in number is 5,000. The discrepancies we consider are Total Variation, Hellinger Distance and KL divergence and  $\alpha$ -divergence with  $\alpha = 2$ . The true values of the discrepancies are obtained by Monte Carlo method with  $10^8$  samples.

**1-dimensional examples.** The densities are defined as below and the results are summarized in Figure 3.

$$p_1(x) = \beta_{6,5}(x), p_2(x) = \beta_{5,6}(x)$$

**3-dimensional examples.** The densities are defined as below and the results are summarized in Figure 4.

$$p_1(x, y, z) = \frac{2}{5}\beta_{1,2}(x)\beta_{2,3}(y)\beta_{3,4}(z) + \frac{3}{5}\beta_{4,3}(x)\beta_{3,2}(y)\beta_{2,1}(z)$$

$$p_2(x, y, z) = \frac{2}{5}\beta_{1,3}(x)\beta_{3,5}(y)\beta_{5,7}(z) + \frac{3}{5}\beta_{7,5}(x)\beta_{5,3}(y)\beta_{3,1}(z)$$

**Bias and Variance Tradeoff.** The vanishing boundaries of beta distribution cause the large range and variance of KL and  $\alpha$  divergence where division is involved, which is undesirable in some applications. We propose two approaches to reduce variance from the *Bias and Variance Tradeoff* perspective:

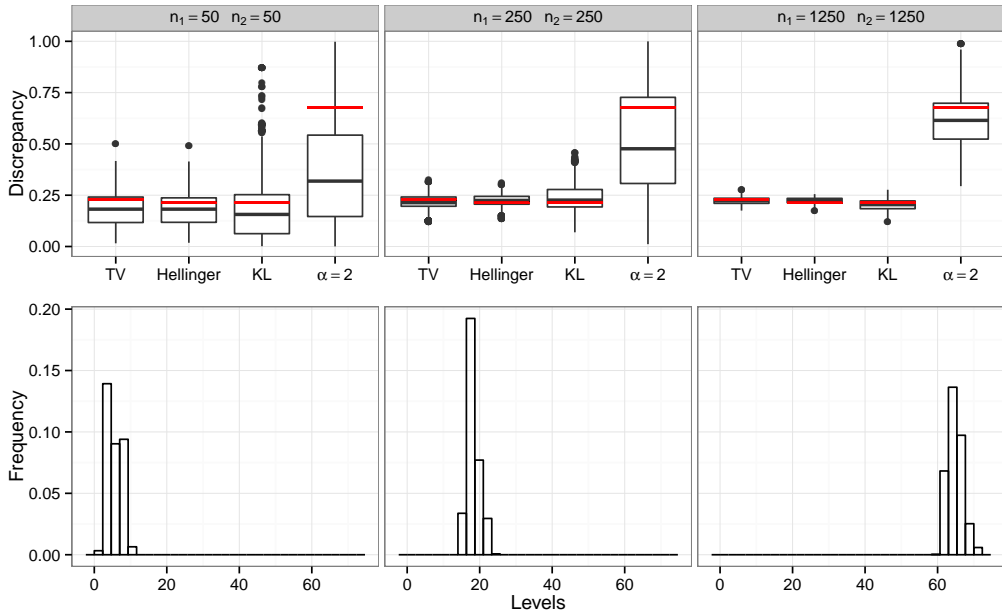


Figure 4: **3-dimensional simulation.** First row, box-plot with the same configuration as 1-dimensional case; theoretical discrepancies (red lines): 0.2301, 0.2129, 0.2133, 0.6769. Second row, we assess the behavior of level  $l$  after discarding first 5,000 burn-in samples, it is obvious that the distribution of  $l$  concentrates on a very small range and is rather peaky.

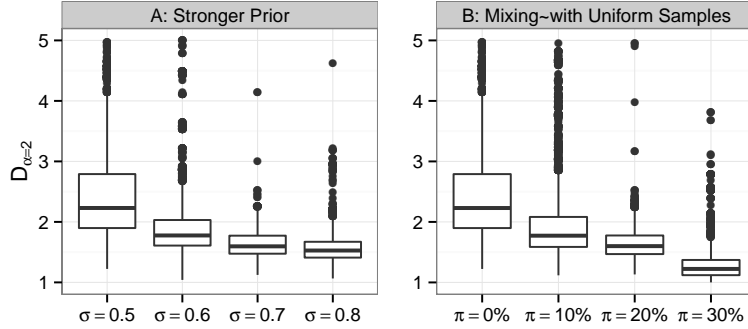


Figure 5: **Illustration of bias and variance tradeoff.**  $\mathcal{X} \sim \mathcal{N}(\mu_1 \mathbf{1}, \Sigma_1 \mathbf{I})$ ,  $\mathcal{Y} \sim \mathcal{N}(\mu_2 \mathbf{1}, \Sigma_2 \mathbf{I})$  and are truncated in  $[0, 1]^4$ , where  $|\mathcal{X}| = |\mathcal{Y}| = 500$ ;  $\mu_1 = 1/3, \mu_2 = 1/2$  and  $\Sigma_1 = 1/5, \Sigma_2 = 1/5$ ;  $\mathbf{1}$  is 4-dim unit vector and  $\mathbf{I}$  is 4-dim identity matrix. As pseudo-count  $\sigma$  or percentage  $\pi$  increases, the variance decreases and bias increases. True value: 2.2196.

- **imposing a stronger prior.** Instead of using Jeffrey’s noninformative prior, we choose a stronger prior with larger  $\sigma$ . The intuition is by law of total variance. For example,  $\text{Var}(m_{1i}) = E[\text{Var}(m_{1i}|\mathcal{X})] + \text{Var}[E(m_{1i}|\mathcal{X})]$ . Since  $m_{1i}$  is generated from Dirichlet distribution,  $\text{Var}(m_{1i}|\mathcal{X}) = \frac{(n_{1i} + \sigma)(n_1 + \sigma l - n_{1i} - \sigma)}{(n_1 + \sigma l)^2 (n_1 + \sigma l + 1)} = O(\sigma^{-1})$  and  $\text{Var}[E(m_{1i}|\mathcal{X})] = \text{Var}\left(\frac{n_{1i} + \sigma}{n_1 + \sigma l}\right) = \frac{\text{Var}(n_{1i})}{(n_1 + \sigma l)^2}$ ; thus, asymptotically, its variance is reduced with a larger  $\sigma$ .
- **mixing with uniform samples.** Given a percentage  $\pi$  (e.g., 10%), generating samples  $\mathcal{X}'$  and  $\mathcal{Y}'$  from uniform distribution such that  $|\mathcal{X}'| \approx \pi|\mathcal{X}|$  and  $|\mathcal{Y}'| \approx \pi|\mathcal{Y}|$  and creating  $X = \mathcal{X} \cup \mathcal{X}'$  and  $Y = \mathcal{Y} \cup \mathcal{Y}'$ . Hence,  $X$  and  $Y$  can be regarded as samples generated from  $\bar{p}_1 \sim p_1 + \pi \mathbf{1}$  and  $\bar{p}_2 \sim p_2 + \pi \mathbf{1}$  respectively, both  $\bar{p}_1$  and  $\bar{p}_2$  are strictly bounded away from 0.

**Higher Dimensional Examples and Comparisons.** There are few higher dimensional experiments in previous work, we demonstrate two additional examples with  $d = 5, 10$  and assess the convergence rate empirically. As shown in Figure 6, the sample size is plotted



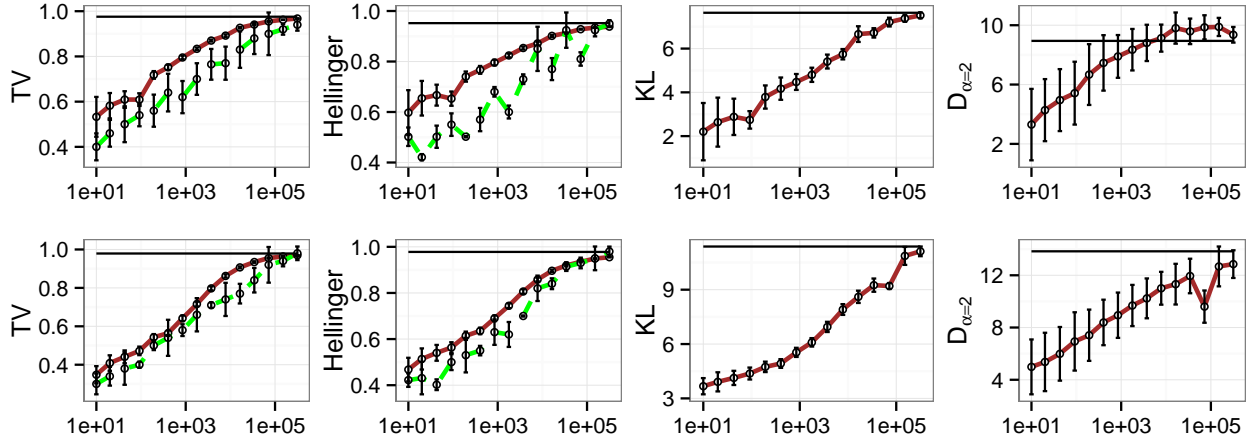


Figure 6: **Higher dimensional examples and comparison.**  $\log(\text{Sample size})$  vs. Discrepancies. Brown solid curves are estimation of discrepancies by our algorithm and green dashed curve are estimation of discrepancies by kernel density estimation (KDE). Top: 5-dim example, the true values of Total Variation, Hellinger Distance, KL divergence and  $\alpha$ -divergence with  $\alpha = 2$  are 0.9756, 0.9520, 7.6365, 8.9440 respectively. Bottom: 10-dim example, the true values are 0.9790, 0.9779, 11.3819, 13.8341. We do not draw KL and  $\alpha$  divergence curves for KDE since their values are too sensitive to bandwidth selection and range quite wildly in our experiments, which is related to the existence of the division term.

on the log scale and the error bars are standard deviation of Monte Carlo samples. There are two important observations: (1) on the log scale, the estimates converge to true values almost linearly, which is comparable to the results in [9]; (2) the estimates in lower dimensions converge relatively faster than those in higher dimensions, this high dimension degradation corroborates the already cited work, which corresponds to the difficulty in multivariate density estimation. As a comparison, we use kernel density estimator for  $p_1$  and  $p_2$  independently and then use Monte Carlo methods to estimate  $D$  on the same settings. We choose RBF kernel and use the package by [5] to do bandwidth selection.

$$p_1(x) = \frac{24}{25} \prod_{i=1}^d \beta_{1,5}(x_i) + \frac{1}{25} \mathbf{1}\{x \in [0, 1]^d\}, p_2(x) = \frac{49}{50} \prod_{i=1}^d \beta_{5,1}(x_i) + \frac{1}{50} \mathbf{1}\{x \in [0, 1]^d\}$$

## 6 Conclusion and Discussion

A unified approach to estimating discrepancies of distributions is proposed from a Bayesian perspective. The joint prior provides a single-shot way to estimate the values and conduct statistical inferences; the simulations demonstrate its attractive empirical performance. In applications, this approach can be naturally extended to handle multiple-sample case jointly. The core of our methodology is Theorem 1, which opens up the possibility to apply any domain partition based density estimators, for instance, Yang et al. [17] proposes a density estimator via adaptive partition and discrepancy control and analyzes its finite sample performance, a possible future direction is to extend their algorithm and error analysis to compare two samples.

## References

- [1] S. Ali and S. D. Silvey. A general class of coefficients of divergence of one distribution from another. *Journal of the Royal Statistical Society. Series B (Methodological)*, pages 131–142, 1966.
- [2] K. Chaloner and I. Verdinelli. Bayesian experimental design: A review. *Statistical Science*, 10(3):273–304, 1995.
- [3] W. K. Hastings. Monte carlo sampling methods using markov chains and their applications. *Biometrika*, 57(1):97–109, 1970.
- [4] P. J. M. P. P. Ho and N. Vasconcelos. A kullback-leibler divergence based kernel for svm classification in multimedia applications. *Proc Adv Neural Inf Process Syst*, 16:1385–1392, 2004.

- [5] M. Kristan, A. Leonardis, and D. Skočaj. Multivariate online kernel density estimation with gaussian kernels. *Pattern Recognition*, 44(10):2630–2642, 2011.
- [6] N. Leonenko, L. Pronzato, and V. Savani. A class of rényi information estimators for multidimensional densities. *The Annals of Statistics*, 36(5):2153–2182, 2008.
- [7] F. Liang, C. Liu, and R. Carroll. *Advanced Markov chain Monte Carlo methods: learning from past samples*, volume 714. John Wiley & Sons, 2011.
- [8] L. Ma and W. H. Wong. Coupling optional pólya trees and the two sample problem. *Journal of the American Statistical Association*, 106(496), 2011.
- [9] X. Nguyen, M. J. Wainwright, and M. I. Jordan. Estimating divergence functionals and the likelihood ratio by convex risk minimization. *Information Theory, IEEE Transactions on*, 56(11):5847–5861, 2010.
- [10] B. Póczos and J. G. Schneider. On the estimation of alpha-divergences. In *International Conference on Artificial Intelligence and Statistics*, pages 609–617, 2011.
- [11] A. Rényi. On measures of entropy and information. In *Fourth Berkeley Symposium on Mathematical Statistics and Probability*, pages 547–561, 1961.
- [12] R. Sainudiin, G. Teng, J. Harlow, and D. Lee. Posterior expectation of regularly paved random histograms. *ACM Transactions on Modeling and Computer Simulation (TOMACS)*, 23(1):6, 2013.
- [13] K. Sricharan, R. Raich, and A. O. Hero III. Empirical estimation of entropy functionals with confidence. *arXiv preprint arXiv:1012.4188*, 2010.

- [14] M. Sugiyama, T. Kanamori, T. Suzuki, M. C. du Plessis, S. Liu, and I. Takeuchi. Density-difference estimation. In *NIPS*, volume 25, pages 692–700, 2012.
- [15] Q. Wang, S. R. Kulkarni, and S. Verdú. Divergence estimation of continuous distributions based on data-dependent partitions. *Information Theory, IEEE Transactions on*, 51(9):3064–3074, 2005.
- [16] Q. Wang, S. R. Kulkarni, and S. Verdú. Divergence estimation for multidimensional densities via-nearest-neighbor distances. *Information Theory, IEEE Transactions on*, 55(5):2392–2405, 2009.
- [17] K. Yang and W. H. Wong. Density estimation via adaptive partition and discrepancy control. *arXiv preprint arXiv:1404.1425*, 2014.

## A Proof of Theorem 1

*Proof.* For  $D_\phi$ , we decompose the integral by  $\{r_{1,l}, \dots, r_{l,l}\}$  and apply Jensen's inequality,

$$\begin{aligned} D_\phi(p_1, p_2) &= \int_{\Omega} p_1(x) \phi\left(\frac{p_2(x)}{p_1(x)}\right) dx = \sum_{i=1}^l \int_{r_{i,l}} p_1(x) \phi\left(\frac{p_2(x)}{p_1(x)}\right) dx \\ &= \sum_{i=1}^l P_1(r_{i,l}) E_{p_1(\cdot|r_{i,l})} \left[ \phi\left(\frac{p_2(x)}{p_1(x)}\right) \right] \geq \sum_{i=1}^l P_1(r_{i,l}) \phi\left( E_{p_1(\cdot|r_{i,l})} \frac{p_2(x)}{p_1(x)} \right) = \sum_{i=1}^l P_1(r_{i,l}) \phi\left( \frac{P_2(r_{i,l})}{P_1(r_{i,l})} \right) \end{aligned} \quad (8)$$

For  $D_\alpha$ , when  $0 < \alpha < 1$ ,  $x^{1-\alpha}$  is concave,

$$\int_{r_{i,l}} \frac{p_1(x)^\alpha}{p_2(x)^{\alpha-1}} dx = P_1(r_{i,l}) E_{p_1(\cdot|r_{i,l})} \left( \frac{p_2(x)}{p_1(x)} \right)^{1-\alpha} \leq P_1(r_{i,l}) \left( E_{p_1(\cdot|r_{i,l})} \frac{p_2(x)}{p_1(x)} \right)^{1-\alpha} = \frac{P_1(r_{i,l})^\alpha}{P_2(r_{i,l})^{\alpha-1}}$$

when  $\alpha > 1$ ,  $x^\alpha$  is convex,

$$\int_{r_{i,l}} \frac{p_1(x)^\alpha}{p_2(x)^{\alpha-1}} dx = P_2(r_{i,l}) E_{p_2(\cdot|r_{i,l})} \left( \frac{p_1(x)}{p_2(x)} \right)^\alpha \geq P_2(r_{i,l}) \left( E_{p_2(\cdot|r_{i,l})} \frac{p_1(x)}{p_2(x)} \right)^\alpha = \frac{P_1(r_{i,l})^\alpha}{P_2(r_{i,l})^{\alpha-1}}$$

thus, in both cases,

$$D_\alpha(p_1, p_2) \geq \frac{1}{\alpha-1} \log \sum_{i=1}^l \frac{P_1(r_{i,l})^\alpha}{P_2(r_{i,l})^{\alpha-1}}$$

For  $D_q$ , when  $q = 1$ ,

$$\int_{r_{i,l}} |p_1(x) - p_2(x)| dx \geq \left| \int_{r_{i,l}} p_1(x) dx - \int_{r_{i,l}} p_2(x) dx \right| = \left| P_1(r_{i,l}) - P_2(r_{i,l}) \right|$$

when  $q = 2$ , we apply Cauchy-Schwarz inequality,

$$\begin{aligned} \int_{r_{i,l}} (\sqrt{p_1(x)} - \sqrt{p_2(x)})^2 dx &= \int_{r_{i,l}} (p_1(x) + p_2(x)) dx - 2 \int_{r_{i,l}} \sqrt{p_1(x)p_2(x)} dx \\ &\geq P_1(r_{i,l}) + P_2(r_{i,l}) - 2 \sqrt{\int_{r_{i,l}} p_1(x) dx} \sqrt{\int_{r_{i,l}} p_2(x) dx} = (\sqrt{P_1(r_{i,l})} - \sqrt{P_2(r_{i,l})})^2 \end{aligned} \tag{9}$$

Sum over  $i$ , the theorem follows. □